REVIEW

Two-Dimensional Electronic Spectroscopy with Active Phase Management†

Wei-da Zhu[a], Rui Wang[a], Xiao-yong Wang[a], Min Xiao[a,b], Chun-feng Zhang[a]*

a. National Laboratory of Solid State Microstructures, School of Physics, and Collaborative Innovation Center for Advanced Microstructures, Nanjing University, Nanjing 210093, China
b. Department of Physics, University of Arkansas, Fayetteville, Arkansas 72701, United States of America

(Dated: Received on December 31, 2020; Accepted on January 29, 2021)

Two-dimensional electronic spectroscopy (2DES) is a powerful method to probe the coherent electron dynamics in complicated systems. Stabilizing the phase difference of the incident ultrashort pulses is the most challenging part for experimental demonstration of 2DES. Here, we present a tutorial review on the 2DES protocols based on active phase managements which are originally developed for quantum optics experiments. We introduce the 2DES techniques in box and pump-probe geometries with phase stabilization realized by interferometry, and outline the fully collinear 2DES approach with the frequency tagging by acoustic optical modulators and frequency combs. The combination of active phase managements, ultrashort pulses and other spectroscopic methods may open new opportunities to tackle essential challenges related to excited states.

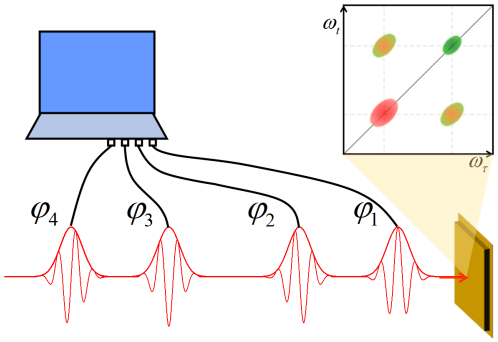

Key words: Two-dimensional electronic spectroscopy, Active phase management, Frequency comb

I. INTRODUCTION

Along with the development of ultrafast laser technology, time-resolved spectroscopy has achieved great success in characterizing the excited-state dynamics in various systems of fundamental significance and technical importance. Ultrashort pulses with few-cycle temporal durations have become available for spectroscopic measurements, which, in principle, can provide temporal resolution sufficient for probing the coherent electronic dynamics in complex and condensed systems at room temperature. However, the broad spectral coverages of ultrashort pulses make it challenging to simultaneously achieve high resolutions in time and excitation-energy domains. This issue can be circumvented with two-dimensional Fourier transform (2D FT) spectroscopy by adding a new excitation frequency dimension. 2D FT spectroscopy probes third-order nonlinear optical response as a function of the time intervals of three incident pulses (FIG. 1). By Fourier transformation, the optical response is then analyzed in the domains of excitation and emission energies with high temporal resolution in population delays.

The early implementation of 2D FT spectroscopy is in the infrared region [1, 2]. To date the frequency range of 2D FT spectroscopy has been expanded from ultraviolet [3−15] to terahertz frequencies [16, 17]. Prospects and potential applications of these cutting-edge technologies have been widely discussed [2, 18−27]. Here we restrict our discussion within the scope of 2D FT spectroscopy in the visible and near-infrared region, *i.e.* two-dimensional electronic spectroscopy (2DES). 2DES

†Part of special topic of "the New Advanced Experimental Techniques on Chemical Physics".
*Author to whom correspondence should be addressed. E-mail: cfzhang@nju.edu.cn

provides insight about coherent electronic dynamics by correlating the initial absorption frequencies with subsequent changes along the emission frequency axis. It enables identification of coupling between different excited states in ensembles by disentangling the homogeneous and inhomogeneous linewidths of electronic transitions. In the past decade, 2DES has been proved to be powerful to study the excited-state dynamics and the coherent coupling of electronic and vibrational degree of freedoms in a variety of photo-activated systems, such as photosynthetic complexes [28−34], molecular aggregates [35], and inorganic semiconductors [36, 37, 38−40].

Technically, phase management is the most challenging part for 2DES measurements. To stabilize the phase differences between the incident ultrashort pulses, passive and active phase locking techniques have been introduced in the last decade. Passive phase managements based on pulse shaper, diffraction optics and other pairwise configurations have been commonly used in the community of physical chemistry as summarized in available review papers [18, 20, 41]. Nevertheless, much less attention has been paid on the 2DES methods with active phase managements. In this review, we intend to give an introduction of the state-of-art 2DES approaches realized with active phase managements. We first introduce the 2DES techniques in box and pump-probe geometries with phase stabilization realized by interferometry. Then we outline the fully collinear 2DES approach with the frequency tagging by acoustic optical modulators (AOMs) and frequency combs. Finally, we will give a brief outlook for the development of 2DES in the future.

II. PRINCIPLES OF 2DES

As shown in FIG. 1(a), 2DES analyzes the four-wave-mixing (FWM) signal generated by three sequenced pulses with variable time intervals. In the perturbation approximation, the signal field $E_{\rm sig}^{(3)}(t)$ emitted by the third-order nonlinear polarization $P^{(3)}(t)$ could be written as

$$E_{\rm sig}^{(3)}(t) \propto iP^{(3)}(t) \propto \int_0^\infty {\rm d}t_3 \int_0^\infty {\rm d}t_2 \int_0^\infty {\rm d}t_1 E_3(t-t_3)E_2(t-t_3-t_2)E_1(t-t_3-t_2-t_1)R^{(3)}(t_3,t_2,t_1) \quad (1)$$

The third-order nonlinear response function could be written as

$$R^{(3)}(t_3,t_2,t_1) \propto \langle \hat{\mu}(t_3+t_2+t_1)[\hat{\mu}(t_2+t_1),[\hat{\mu}(t_1),[\hat{\mu}(0),\rho(-\infty)]]]\rangle \quad (2)$$

In Eq.(2), $\rho(-\infty)$ represents the initial density matrix of the system. The three transition diploe operators $\hat{\mu}(0)$, $\hat{\mu}(t_1)$, and $\hat{\mu}(t_2{+}t_1)$ embraced in the nested commutators represent the three consecutive interactions with the sequenced excitation pulses, but the fourth transition diploe operator $\hat{\mu}(t_3+t_2+t_1)$ represents the emission of signals. Ideally, the excitation laser pulses are expected to be short enough compared to any timescale of the system, but long enough compared to the oscillation period of the light field. In this so-called semi-impulsive limit, the signal field would be approximately proportional to the response function as

$$E_{\rm sig}^{(3)}(t) \propto R^{(3)}(t,T,\tau) \quad (3)$$

Now, we could briefly describe the time evolution of the system interacted with the excitation pulses and the generation of the third-order signal field. For one-quantum 2DES experiments, the first pulse 1 interacts with the system and creates a coherence between the ground and excited state. After a coherence time delay τ, the system is switched to a population state through the interaction with the second pulse 2. The third pulse 3 then puts the system in a coherent state again after a waiting time delay T. The time period during which the FWM signal is emitted is denoted as t. A 2D spectrum for a given waiting time T can be acquired if the recorded FWM signal is Fourier transformed in the domains of τ and t delays. In practice, to reduce the data acquisition time, the relatively weak FWM signal is typically heterodyne detected using a local oscillator and

DOI:10.1063/1674-0068/cjcp2012222

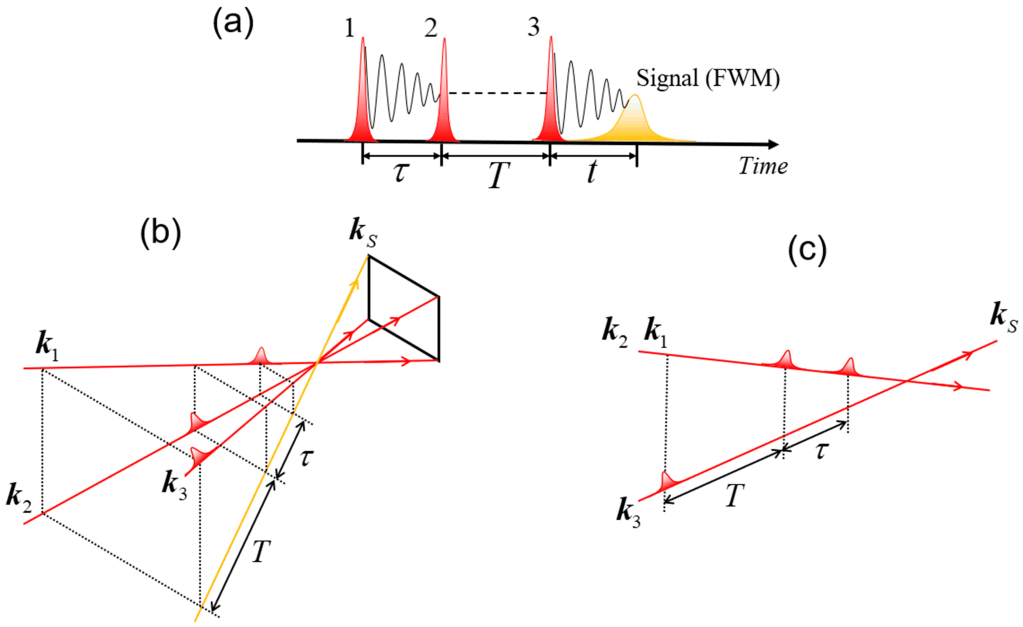

FIG. 1 Schematic diagram of pulse sequence for 2DES. (a) The time order of the three excitation pulses and the generated four-wave mixing signal. (b) The fully non-collinear box geometry and (c) the partially collinear pump-probe geometry.

analyzed by a spectrometer. For different sequences of the first two pulses, 2DES captures the rephasing signal ($\boldsymbol{k}_{\mathrm{R}}=-\boldsymbol{k}_1+\boldsymbol{k}_2+\boldsymbol{k}_3$) and the non-rephasing signal ($\boldsymbol{k}_{\mathrm{NR}}=\boldsymbol{k}_1-\boldsymbol{k}_2+\boldsymbol{k}_3$), where $\boldsymbol{k}_i$ denotes the wave vector of the ith pulse interacting with the system. A pure absorptive 2D signal can be acquired by summing the rephasing and non-rephasing signals. The absorptive 2D spectra are most frequently used because they are free from broadening refractive contributions and can be directly regarded as an extension of transient absorption spectra along an additional excitation frequency axis. Another 2D signal related to two-quantum coherence can be captured in the phase-matching direction $\boldsymbol{k}_1+\boldsymbol{k}_2-\boldsymbol{k}_3$ [22], where the system is put in a coherence between the ground and double excited states in a two-quantum excitation scheme. Experimentally, three different geometries have been employed for 2DES measurements. In the most widely used box geometry (FIG. 1(b)), 2D signals corresponding to different phase matching conditions can be detected in the same direction by changing the time-ordering of the pulses. These phase matched signals are almost background free since they are spatially separated from the excitation pulses so that relatively high signal-to-noise ratio is achievable. Moreover, the ability to individually manipulate the excitation pulses in this geometry enables polarization-based signal selection and further background suppression. For the pump-probe geometry (FIG. 1(c)), the collinear alignment of the first two pulses makes it challenging to disentangle the rephasing and non-rephasing signals. Nonetheless, the sum of the rephasing and non-rephasing pathways provides the correlation 2D signal with absorptive and dispersive signals. In comparison with the conventional transient absorption spectroscopy that captures the photo-excited absorption change related to the population occupied at the excited states, 2DES probes the absorption change as a function of the time interval between the first two incident pulses. In addition, a fully collinear geometry has also been recently used for 2DES, which is of particular meaning for implementation with microscopy. As shown in FIG. 2(a), 2DES can extract the intrinsic spectral information from inhomogeneous broadening system, which allows to probe the dynamics of excited states with high excitation energy resolution which is hindered by the Fourier transform limit of the ultrashort pulse in transient absorption spectroscopy. Moreover, 2DES captures the information of off-diagonal elements in the population matrix of a complex system that may uncover the coherent coupling between different excited states (FIG. 2(b)).

Phase management is critical for implementation of 2DES. For one-quantum 2DES experiments, the FWM signal field oscillates with respect to delay τ and t at an optical frequency corresponding to the energy difference between the ground and excited states. The time inter-

DOI:10.1063/1674-0068/cjcp2012222

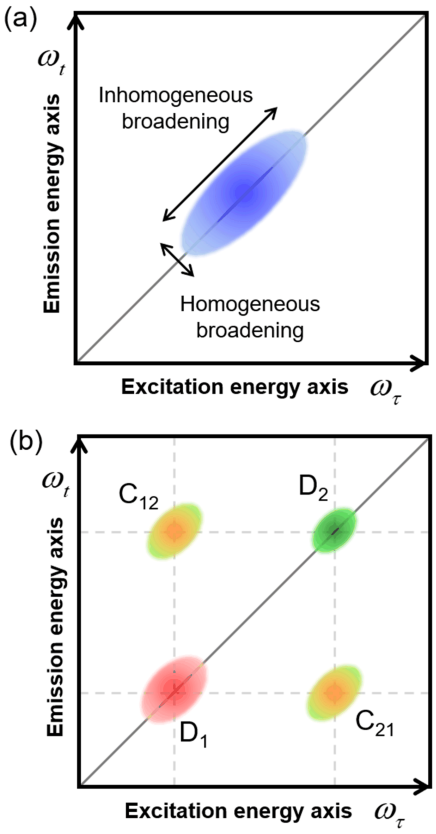

FIG. 2 Schematic one-quantum absorptive 2D spectra for (a) single transition resonance and (b) couple two transition resonances.

vals, usually controlled by mechanical translation stages for pump-probe spectroscopy, should be more precisely controlled with phase stabilized to achieve the accurate value of excitation and emission energies. The phase instability caused by mechanical fluctuation may average out the coherence-related 2D signal. In addition, the spectral coverages of ultrashort pulses used for 2DES measurements are broad to ensure a high temporal resolution. It is essential to control the spectral dispersion of the phase differences of multiple incident ultrashort pulses with different optical paths.

In the past decade, a variety of phase stabilization protocols have been proposed for the implementation of 2DES. Passive methods have been widely adopted in the community of chemical physics. In general, the excitation pulses have been designed to travel along the common paths or inter-related paths to cancel the total phase fluctuations using the strategies including diffractive optics based schemes in the box geometry [42−47], pulse shaper based schemes in both pump-probe [48, 49] and box [50−53] geometries, and Translating-Wedge-Based Identical Pulses eNcoding System (TWINS) based schemes in the pump-probe geometry [54, 55]. Since these passive methods have been detailed in some other comprehensive reviews [18, 20], we will not discuss further here. In contrast, active phase managements for 2DES experiments have been rarely used in the community of chemical physics although the active technique exhibits more robust phase stabilization and enables longer coherence time delay. The barrier is possibly caused by the difficulty in implementation of the phase locking electronics. In the following, we will introduce the active phase management methods including the interferometry-based phase locking, frequency tagging by AOMs, and frequency combs, respectively.

III. INTERFEROMETRY-BASED PHASE MANAGEMENT

The early attempts of 2D FT spectroscopy have employed interferometers to create the sequenced excitation pulses [56, 57]. Nevertheless, mechanical fluctuations usually introduce considerable phase noise when constructing a 2DES apparatus based on interferometers since the delayed pulses are delivered by different mirrors and go through separate paths in the interferometers.

Cundiff and coworkers have established the phase locking with active phase stabilization electronics and succeeded in developing a versatile apparatus for 2D FT measurements, known as the JILA-MONSTER [58]. Two Michelson interferometers are folded and nested to a third larger interferometer to create the four delayed and phase-controlled pulses in a box geometry. All the four generated pulses can be phase stabilized actively using a co-propagating continuous-wave (cw) laser throughout the three interferometers. Hence, in addition to the one-quantum measurements, this setup allows access to two-quantum 2D spectra, which usually contain information of many-body interactions [39, 59−61]. Jonas and coworkers have demonstrated a 2DES scheme in the near-infrared spectral range in the partially collinear pump-probe geometry to selectively detect the absorptive 2D signal [62]. The collinear pump pulse pair is created and phase stabilized from a Mach-Zehnder interferometer enhanced by active feedback electronics. Zhu *et al.* have combined the active phase stabilization and the broadband two-color pump-

DOI:10.1063/1674-0068/cjcp2012222

probe geometry using sub-10 fs pulses in the visible and near-infrared range with precise phase correction [63].

In FIG. 3, we show a brief diagram for the technique of interferometry-based phase management. Briefly, a cw laser beam co-propagates along with the excitation pulses in the interferometer. The interference signal between the cw laser beams in each arm of the interferometer is detected and used as an error signal which reflects the delay fluctuation between the pulse pair. This error signal is fed into an electronic feedback loop that drives a piezoelectric transducer (PZT) attached in one of the arms to compensate the delay fluctuation and the inter-pulse phase is thus actively stabilized. Such an active phase stabilization procedure can reduce the mechanical fluctuation to less than 1 nm, which is generally much better than those of available passive methods. To construct an accurate 2D spectrum, one must complete the data collection procedure when the interferometer is locked. Then the interferometer is unlocked to allow the translation stage to scan the delay τ to a next value. Afterwards, the interferometer is locked again to record the next spectral signal. This process can be controlled and repeated automatically by a computer.

The spectral dispersion of phase difference between the two pump pulses, which can be retrieved from their spectral interferogram monitored by a diagnostic spectrometer, is required for phase correction of 2D spectra. In the passive phase locking scenario, a widely used method for phase retrieval is to compare the obtained 2D signal with a measured spectrally-resolved transient absorption signal according to the projection-slice theorem [22]. Great care should be taken for the phase recovery for the ultrashort pulses with broad spectral coverage in the interferometry-based scenario. In principle, the two pump pulses with zero τ delay have a flat spectral dependence on zero phase difference over the whole spectral range. However, it is generally more complicated since a tiny difference between the optical paths of two arms of the interferometer may cause additional phase distortion. The effect of such phase distortion is significant and cannot be neglected when the bandwidth of the pump pulses is broad. For the interferometer-based approaches (FIG. 3), a slight thickness difference between the quartz substrates of the two beam splitters in the Mach-Zehnder interferometer or a tiny misalignment may cause a dramatic issue on the phase. To avoid this side effect, a pair of wedges and a compensation plate are inserted in the two arms of the interferometer to precisely manipulate the phase difference between the two pump pulses. This capacity of phase control also enables to separate the rephasing and non-rephasing signals in the measurement as inspired by the phase cycling scheme adopted by Ogilvie *et al.* [49]. In consequence, the interferometer-based phase management can disentangle the rephasing and non-rephasing signals with the 2DES based on pump-probe geometry.

In addition to the robust phase stability, 2DES approaches using interferometry-based active management enable long coherence time delays which are only limited by the range of delay lines. Optical elements can be simply implemented in the two arms of interferometers to individually manipulate the amplitudes, spectra, phases and polarizations of each pulses, which is promising for noise suppression and signal isolation. The technique barrier can be easily addressed with commercially available electronics (*e.g.*, LB1005, Newport).

IV. FREQUENCY TAGGING WITH AOMS

For either box or pump-probe geometries, the non-collinear alignment of the excitation beams make it difficult to be integrated with microscopy. Moreover, these non-collinear geometries cannot be applied to probe single nanostructures as the radiation by point sources prevents the formation of a well-defined FWM beam in the phase-matched direction. To tackle this issue, incoherent signals such as fluorescence [64−70], photocurrent [71−73] or photoemission electrons [74−76] combined with the simplest fully collinear geometry have also been successfully used to capture specific nonlinear signals. In principle, the 2DES signals for specific quantum pathways can be analyzed with a response-function treatment [75, 77]. A fully collinear geometry implies that the setup can be integrated with microscope objectives, making spatially resolved 2DES measurements facile.

One strategy to isolate the desired signals in such a collinear geometry is phase cycling, which was first implemented by Warren and co-workers using an AOM based pulse shaper [64]. Different phases between the individual laser pulses of a sequence are modulated in the phase cycling methods and various nonlinear contributions, such as the rephasing and non-rephasing signals, can be retrieved simultaneously by linear superposition of several differently phase-modulated raw data with appropriate weights. However, the data collec-

DOI:10.1063/1674-0068/cjcp2012222

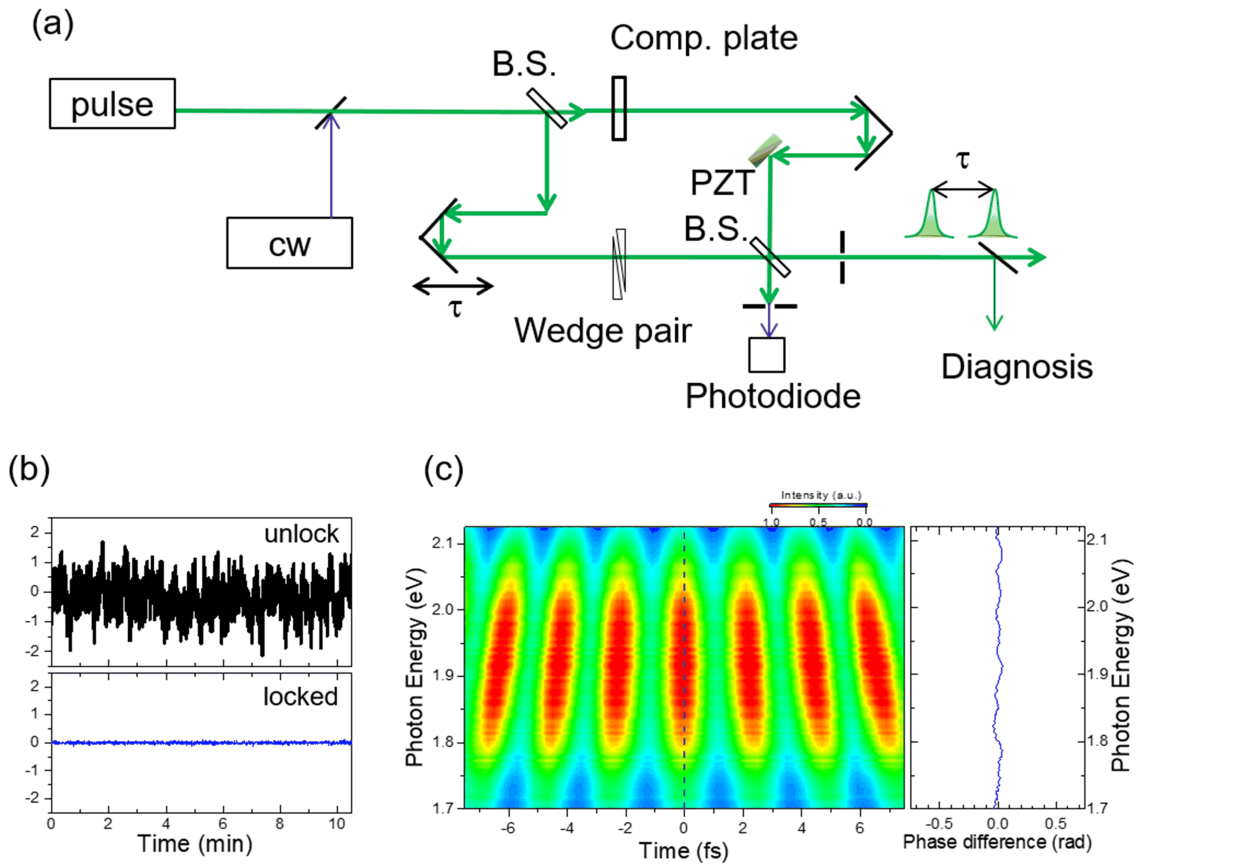

FIG. 3 (a) A schematic diagram for interferometry-based phase management of two ultrashort pulses. BS: beam splitter, PZT: piezoelectric transducer, Comp. plate: compensation plate. (b) The error signals for the interferometer recorded for 10 min without (top) and with (bottom) active stabilization engaged. (c) The interferometer spectra of the two excitation pulses with phase correction. The phase distortion is less than 0.05 rad over the broadband spectral range of the excitation pulses.

tion process is generally tedious for phase cycling. For instance, it usually requires 27 (1×3×3×3) scans with different relative pulse phases to extract a single absorptive 2D spectrum [78], which is problematic for samples with significant photobleaching. To remedy this limitation, Brixner and coworkers customized a pulse shaper to facilitate shot-to shot modulation at the repetition rate of the 1 kHz laser system. In this way, they realized rapid scanning over all time delays and a 2D spectrum can be acquired in about 6 s [70]. Furthermore, they combined the fluorescence-detected 2DES with an immersion-oil microscope objective to establish the novel method of coherent 2D fluorescence microscopy with sub-micro spatial resolution [79], which enables the investigation of microscopic variations in heterogeneous systems.

Instead of phase cycling, an alternative phase tagging approach can be adopted for signal extraction in 2DES experiments with fully collinear geometry. In this case, AOMs can be employed to modulate the beams with different frequency shifts. The inter-pulse delays τ, T and t are controlled with three translation stages. Four AOMs are inserted in each arm of the two interferometers to impart a specific radio-frequency (RF) shift to the four pulses respectively. Each excitation pulse is thus tagged with a unique frequency Ω_i (i=1, 2, 3, 4). The radio-frequency shift is so small compared to the optical carrier frequency of the laser pulse that its impact on the excitation of sample by each single pulse can be ignored. However, if we consider a train of pulses with repetition frequency $f_{\rm rep}$ and enumerate the successive pulses by the index n, the carrier envelope phase of each pulse within the train is dynamically shifted by $n\Omega_i/f_{\rm rep}$. Thus, the nonlinear signals induced by the four pulses (with a set of specific inter-pulse delays τ, T and t) oscillate in real time at the radio frequencies given by sums and differences of the AOM frequencies. A lock-in amplifier which is referenced to a specially

DOI:10.1063/1674-0068/cjcp2012222

constructed waveforms can be used to demodulate the nonlinear signals and to isolate them in the RF domain. The lock-in reference waveforms are generated from the interference of a narrowband selection of the excitation pulses themselves using a pair of monochromators. As is shown in FIG. 4, the beat frequencies of waveform Ref1 and Ref2 are detected on two separate photodetectors as $\Omega_{12}=\Omega_1-\Omega_2$ and $\Omega_{34}=\Omega_3-\Omega_4$. They are further electronically mixed to generate the final reference waveform which oscillates at the difference frequency $\Omega_{\rm R}=\Omega_{34}-\Omega_{12}=-\Omega_1+\Omega_2+\Omega_3-\Omega_4$ for the lock-in detection of rephasing signal, or at the sum frequency $\Omega_{\rm NR}=\Omega_{34}+\Omega_{12}=\Omega_1-\Omega_2+\Omega_3-\Omega_4$ for non-rephasing signal. The beating frequencies of these reference waveforms are analogous to the phase-matching conditions in conventional FWM schemes based on (fully or partially) noncollinear geometry. However, a potential limitation of this phase tagging approach is that it may be difficult to distinguish the third-order signals from those higher order signals. For example, signal contributions from the fourth order population $\Omega_1-\Omega_2+\Omega_3-\Omega_4$ and the six order population $\Omega_1-\Omega_1+\Omega_1-\Omega_2+\Omega_3-\Omega_4$ will oscillate at the same modulated frequency in the RF domain, making the separation between them challenging. This issue can be tackled in the phase cycling approach by increasing the steps of the cycle scheme, as has been demonstrated by the Brixner group very recently [80].

Marcus and coworkers introduced the phase tagging approach to isolate the desired nonlinear signal in the frequency domain without relying on the phase-matching condition of a radiated field [67]. This approach is quite appealing to 2DES experiments on individual nanostructures. A schematic diagram of their instrument is shown in FIG. 4. The simplest fully collinear geometry is employed for the loss of phase-matching. The 800 kHz pulse train from a Ti:Sapphire oscillator is fed into a set of two Mach-Zehnder interferometers nested within a larger Mach-Zehnder interferometer to generate the sequenced four collinear pulses. In contrast to the conventional FWM scheme, the role of the fourth pulse here is to convert the third order polarization into a fourth order population which is detectable in the form of fluorescence signal. The interpulse delays τ, T and t are controlled with three translation stages.

Cundiff group implemented multidimensional coherent optical photocurrent spectroscopy (MD-COPS) of a semiconductor nanostructure based on a similar phase tagging scheme [72]. They choose to detect the fourth order population in the form of a photocurrent signal considering inefficient fluorescence from the semiconductor sample. In comparison with the apparatus of Marcus group, they generate the lock-in reference waveforms from the interference of a cw laser co-propagating along the same path of the excitation pulses in the interferometers with a slight vertical shift. The wavelength of the cw laser is selected to be close to the signal wavelength to compensate for phase noise resulting from mechanical fluctuations in the setup. They also point out the phase tagging approach can also be seen as a dynamic phase cycling method and is particularly suitable for 2DES with high-repetition-rate laser sources. In other words, the phase cycling happens in "real time" as each AOM sweeps the carrier-envelope phase over the laser pulse train. This obviates the need for combining multiple separate phase scans to extract the desired signals. Compared with the phase cycling scheme based on a pulse shaper [64], the phase tagging approach usually allows much larger scanning range of coherence time delay, which is limited only by the resolution of the monochromators (Marcus group) or by the coherence length of the cw laser (Cundiff group) when the length of the delay stages are sufficient. This is particularly useful for the 2DES of nanostructures whose coherence time can be on the nanosecond scale.

Ogilvie and coworkers developed a fluorescence-detection-based fully collinear two-dimensional electronic microscopy with femtosecond time resolution and sub-micron spatial resolution [68]. In contrast to the pulse shaper based phase cycling approach adopted by the Brixner group mentioned above, the use of phase tagging approach and lock-in detection enables the use of high-repetition-rate lasers compatible with imaging applications and produces high signal-to-noise ratio images. To demonstrate their approach, they performed *vivo* measurements on a mixture of photosynthetic bacteria and resolved spatially varying excitonic structure due to different growth conditions. They estimated nearly six orders of magnitude fewer bacterial cells contribute to the signal in their fluorescence detection measurements compared to the conventional 2D measurements based on the detection of a radiated electric field.

The phase tagging approach provides some unique advantages. First, the lock-in amplifier filters the input signals over a narrow frequency range centered at the beating frequency tagged on the desired signal so

DOI:10.1063/1674-0068/cjcp2012222

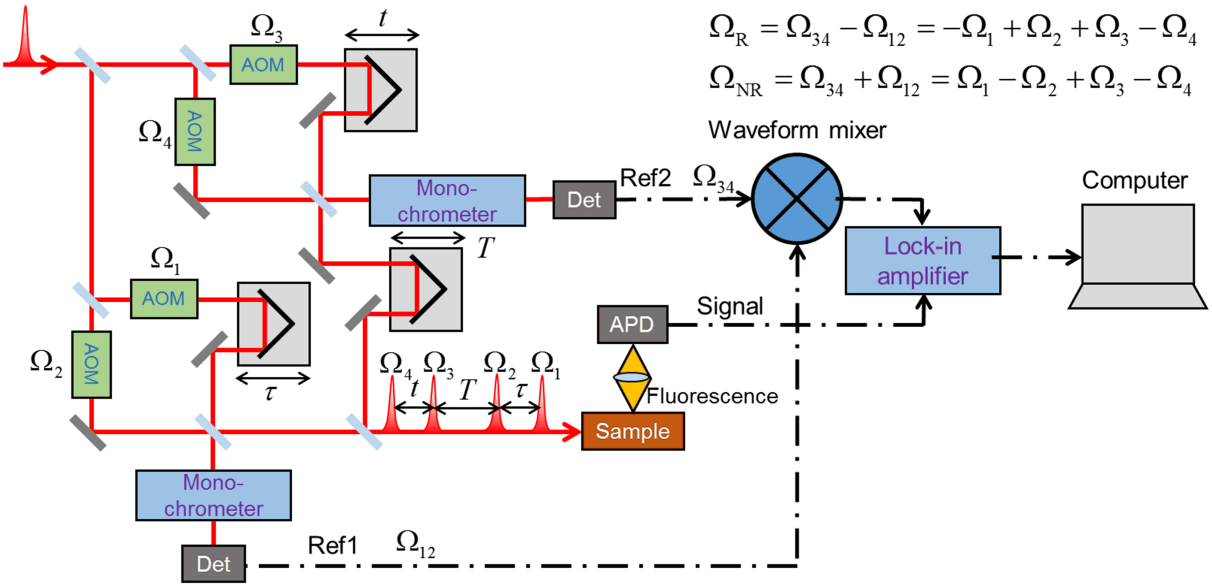

FIG. 4 The optical design of a 2DES setup based on phase modulation with AOMs. Ref: reference, Det: detector, APD: avalanche photodiode.

that a relatively high signal to noise ratio (SNR) can be achieved. Besides, the real and imaginary parts of the complex signal are intrinsically and directly accessible from the in-phase and in-quadrature outputs of the lock-in amplifier because the phase of the signal is correlated to the phase of the excitation pulses involved in the corresponding reference waveform. Moreover, in contrast to the box geometry that rephasing and non-rephasing signals are recorded separately since they correspond to a different pulse sequences, one can collect the two different signals simultaneously on a two-channel lock-in amplifier. Finally and most importantly, just like the sampling mode adopted in the phase cycling methods [64, 70, 78], the desired nonlinear signal is measured in a rotating frame 2 since the phases of the reference signal and the detected nonlinear signal will evolve at similar optical frequencies along with the scanning of coherence delay τ. As a result, the phase of the recorded signal output from the lock-in amplifier will no longer evolve at an optical frequency with delay τ, but at a reduced frequency given by the difference between optical frequencies of the signal and the selected reference wavelength by the monochromators. As a consequence, the signal is physically under sampled with the coherence time and the universal phase noise in 2DES based on interferometers introduced by mechanical fluctuation is largely compensated through the lock-in detection process. The phase of the detected signal is actively stabilized by AOMs without the integration of feedback electronics mentioned in the previous section, reducing the technical barriers to some extent.

V. FREQUENCY COMB-BASED 2DES

In spite of many advantages of the frequency tagging approach on implementing 2DES mentioned above, a main drawback is the requirement of an additional motorized time delay t to be scanned and numerically Fourier transformed to get the emission frequency axis of the 2D spectrum. This is significantly more time-consuming than the conventional schemes where the FWM signal is heterodyne detected with a local oscillator and instrumentally Fourier transformed by a spectrometer. The drawback makes it extremely challenging to study the systems with long dephasing time.

Inspired by the technique of dual-comb spectroscopy (DCS) [81−83], Cundiff and coworkers have developed a compact apparatus for multidimensional coherent spectroscopy based on two frequency combs, which simultaneously provides the highest spectral resolution to date and short acquisition time [84, 85]. The innovation of the DCS method lies in the replacement of the moving mechanical stage, which limits the acquisition speed, with the use of two-phase locked frequency combs with slightly different repetition rates. One comb is employed to interrogate the sample and generate the nonlinear optical signal, while another comb is used as

DOI:10.1063/1674-0068/cjcp2012222

the local oscillator. The subtle repetition rate difference between the two combs equivalently provides a rapid scanning of time delay between the signal pulses and the local oscillator pulses, which is referred to as asynchronous optical sampling (ASOPS) [81, 86]. The signal comb is multi-heterodyne detected through the interference with the local oscillator comb, and then a corresponding beating frequency comb usually located in the RF domain is generated, which directly maps to the signal spectrum in the optical-frequency domain. The beating signal can be detected in the time domain by a photodetector and then be numerically Fourier transformed to recover the RF comb, which can afterwards be rescaled to the optical-frequency domain and recover the desired spectrum with high spectral resolution. The resolution is limited only by the bandwidth of the comb teeth theoretically.

FIG. 5 shows how to integrate the technique of one-dimension DCS into 2DES. We can find in FIG. 5(a) that the laser source of the 2DES setup contains a signal comb and a local oscillator (LO) comb with repetition frequencies f_{Sig} and f_{LO}=f_{Sig}+Δ respectively. The signal comb is split into two parts. One of them is modulated by an AOM to shift its offset frequency by Ω and then is recombined with the other part at a time delay τ controlled by a mechanical delay stage. Thus a sequence of excitation pulses in a collinear geometry is generated to interrogate the sample. The FWM signals emitted from the sample co-propagate with the linear signals from the incident pulses and then are combined with the LO comb. The beating signals are recorded by a photodetector in the time domain corresponding to the mixed linear and FWM signals and then are Fourier transformed to recover the counterparts of the signal combs in the RF domain. The multi-heterodyne detection process is illustrated in the optical and radio-frequency domain in FIG. 5(b). We can find that the spectra of the linear signals (red and purple teeth) and one of the FWM signals (yellow teeth) corresponding to a specific excitation sequence [85] overlap with each other in the optical-frequency domain. However, the spectra of their counterparts in the RF domain are totally separated. In contrast to the complex phase cycling methods, the simple bandpass filtering in the RF domain is enough to isolate the desired FWM signal with high spectral resolution. A 2D spectrum can be constructed after Fourier transformation of the recovered FWM signal with respect to the time delay τ

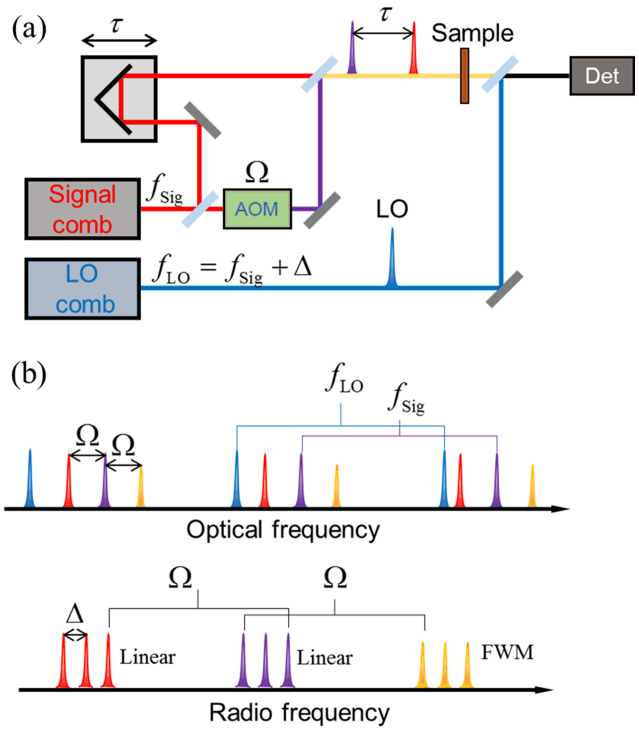

FIG. 5 (a) The optical design and (b) the isolation of the FWM signal in the radio frequency domain. Det: detector.

scanned by the delay stage. Finally, the phase noise of the detected FWM signal must be monitored and corrected, or the FWM comb teeth in the RF domain will be broadened, resulting in a decrease of spectral resolution. Similar to other 2DES schemes based on interferometers, the relative optical path fluctuations will contribute to the phase noise. However, considering the two different laser sources employed in this scheme, phase noise could also arise from the fluctuating offset frequencies and residual relative repetition frequency fluctuations of the two combs. A cw laser co-propagating with the excitation pulses and a well-designed signal process circuit are integrated into the apparatus to measure and cancel these phase fluctuations.

To demonstrate the capability of frequency resolution of their method, they performed 2DES conceptual experiment on a mixture of two naturally occurring isotopes of rubidium atoms (^{87}Rb and ^{85}Rb) [85]. The laser pulses were optically filtered to excite the D_1 lines of Rb atoms, whose natural linewidths of the hyperfine lines are only ~6 MHz, yet Doppler-broadened to 580 MHz at 110 °C. However, along the cross-diagonal direction of the collected 2D spectrum, the inhomogeneous (Doppler) broadening is removed and the line

DOI:10.1063/1674-0068/cjcp2012222

shapes reflect the homogeneous linewidth. Thus the hyperfine structure is successfully resolved without implementing the complex laser cooling apparatus. In addition, the unique locations of the coupling peaks in the 2D spectrum allow assignment of the clustered features between ^{87}Rb and ^{85}Rb.

In their experiment above, a 2D spectrum was obtained in less than 4 min. This acquisition speed is rapid enough compared with the conventional frequency tagging approach due to the replacement of the mechanical stage along t with a second frequency comb. What's more, the Cundiff group further improved the acquisition speed by using a third frequency comb with another different repetition frequency to replace the AOM and the mechanical stage along τ in the experiment [87, 88]. Such a tri-comb 2D coherent spectroscopy employs only a single photodetector and no mechanical stages to enable extremely rapid acquisition speed, while providing comb resolution along both the excitation (absorption) and emission axes. The ^{87}Rb and ^{85}Rb isotopes were again used to test the tri-comb setup. They reproduced the same results as those from the dual-comb setup but with better cross-diagonal resolution and less acquisition time of under 1 s. These improvements make 2DES relevant for atomic systems and field deployable for chemical-sensing application if implemented using compact lasers.

In contrast to the collinear geometry adopted by the Cundiff group, Cho and coworkers proposed a dual frequency comb based photon echo spectroscopy in a noncollinear geometry to spatially separate the FWM signal [89]. With respect to the complicate mapping relation between the optical resonance frequency and the down-converted radio detection frequency, they gave a detailed theoretical analysis of the general dual-comb nonlinear spectroscopy based on the third order response function, which is instructive for experimentalists to design a novel comb-based 2DES setup. Nevertheless, the two-pulse nonlinear spectroscopy schemes mentioned above are not suitable for studying the dynamics of condensed systems because they are limited to the measurement of a 2D spectrum at zero waiting time. Therefore, the Cho group further proposed a three-pulse photon echo spectroscopy with dual frequency combs in a box geometry. The waiting time between the second and third pulse is introduced by employing the ASOPS method and utilizing two independent combs with slightly detuned repetition rates. This ensures uniform data quality over a long population time from the femtosecond to the nanosecond range without the problem of wave front variation that could arise when using mechanical delay stages.

In general, the frequency comb-based 2DES is an emerging technique that can be used to study a variety of molecules both in the gas and condensed phases with unprecedented high frequency resolution and high data acquisition speed. Moreover, the construction of the setup is greatly simplified due to the replacement of the bulky mechanical delay stages and monochromators with different frequency combs and a single photodetector respectively. However, great care should be taken to stabilize the carrier-envelope phases and the repetition rates of the two frequency combs to acquire a precise 2D spectrum experimentally.

VI. SUMMARY AND OUTLOOK

2DES allows to probe the excited-state dynamics with high resolution in the temporal and excitation energy domains simultaneously, which has been established as a powerful tool in elucidating the quantum coherence effect on the electron and energy transfer dynamics. With the emerging methods of phase stabilization and signal isolation, 2DES is becoming a more mature and productive technology available in many laboratories. For experimental implantation, some features are inherent for the configuration geometries. The signals of different pathways can be easily selected by phase matching condition for the fully noncollinear box geometry which, however, requires more efforts on optical design and alignment. The partially collinear pump-probe geometry is probably the most common geometry studying the dynamics excited states. Nevertheless, great care should be taken to subtract the background transient population signal for 2DES based on pump-probe configuration. The fully collinear geometry can be naturally implanted for microscopic measurements, which, however, suffers from entanglement of signals from different pathways. Fuller and Ogilvie have compared the (dis)advantages of different phase matching technique [18]. Here, we briefly summarize the different 2DES approaches based on active phase management (Table I).

Most methods for active phase managements for 2DES are well-established protocols in the community of quantum optics. The marriage of expertise

DOI:10.1063/1674-0068/cjcp2012222

TABLE I Summary of the advantages and disadvantages for 2DES approaches based on active phase management.

Approach	Advantages	Disadvantages
Interferometer with active phase stabilization	Long time robust phase stability Long coherence delay range available Independent manipulation of the excitation pulses in all geometries Capable of two-quantum measurements (box geometry)	Construction complexity from the integration of feedback electronics
Phase modulation (Frequency tagging)	High SNR with lock-in detection Single element detector instead of spectrometer Long coherence delay range available Independent manipulation of the excitation pulses Data acquisition in the rotating frame Especially compatible with high-repetition-rate laser sources	Additional electronics needed to construct reference waveforms Time-consuming due to an additional motorized delay t to be scanned
Frequency comb	Extremely high spectral resolution and rapid data acquisition speed Signal isolation without phase cycling or modulation Simple optical design Single element detector instead of spectrometer Long coherence delay range available	Extra phase noise from the employment of additional laser sources

in the fields of quantum optics and chemical physics may stimulate a rapid development of 2DES technique. 2DES has been successfully combined with microscopy to investigate the single nanostructures. If the spatial resolution can be further improved by combining 2DES with photoelectron emission, scanning near-field spectroscopy, scanning tunneling microscopy and other methods, the structure-coherence correlations in complex systems may become accessible. The combination of frequency-tagged 2DES and mass spectroscopy may be potentially applied to probe the quantum pathways of photochemistry reaction. The frequency comb-based 2DES with ultrahigh spectral resolution may be used to study the fundamental science in the cold atom systems. These potential developments of new methodologies provide cheerful prospect of 2DES in the field of physical chemistry.

VII. ACKNOWLEDGMENTS

This work is supported by the National Key R&D Program of China (No.2017YFA0303700 and No.2018YFA0209101), the National Natural Science Foundation of China (No.21922302, No.21873047, No.11904168, No.91833305, and No.91850105), the Priority Academic Program Development of Jiangsu Higher Education Institutions, and the Fundamental Research Funds for the Central University.

[1] P. Hamm, M. Lim, and R. M. Hochstrasser, J. Phys. Chem. B **102**, 6123 (1998).
[2] P. Hamm and M. Zanni, *Concepts and Methods of 2D Infrared Spectroscopy*, Cambridge: Cambridge University Press, (2011).
[3] T. Chien-Hung, M. Spiridoula, and T. C. Weinacht, Opt. Express **17**, 18788 (2009).
[4] S. Ulrike, S. Carl-Friedrich, F. Michael, L. Florian, N. Patrick, and B. Tobias, Opt. Lett. **35**, 4178 (2010).
[5] C. H. Tseng, P. Sándor, M. Kotur, T. C. Weinacht, and S. Matsika, J. Phys. Chem. A **116**, 2654 (2011).
[6] B. A. West, J. M. Womick, and A. M. Moran, J. Phys. Chem. A **115**, 8630 (2011).
[7] A. Gerald, C. Cristina, V. M. Frank, and C. Majed, Opt. Lett. **37**, 2337 (2012).
[8] B. A. West and A. M. Moran, J. Phys. Chem. Lett. **3**, 2575 (2012).
[9] C. Cristina, A. C. Gerald, V. M. Frank, and C. Majed, Science **339**, 1586 (2013).
[10] N. Krebs, I. Pugliesi, J. Hauer, and E. Riedle, New J. Phys. **15**, 085016 (2013).
[11] B. A. West, P. G. Giokas, B. P. Molesky, A. D. Ross, and A. M. Moran, Opt. Express **21**, 2118 (2013).

DOI:10.1063/1674-0068/cjcp2012222

[12] J. R. Widom, N. P. Johnson, P. H. von Hippel, and A. H. Marcus, New J. Phys. **15**, 5028 (2013).
[13] V. I. Prokhorenko, A. Picchiotti, S. Maneshi, and R. J. D. Miller, *In 19th International Conference on Ultrafast Phenomena*, Okinawa, Japan, Vol. 162, 432 (2014).
[14] R. Borrego-Varillas, A. Oriana, L. Ganzer, A. Trifonov, I. Buchvarov, C. Manzoni, and G. Cerullo, Opt. Express **24**, 28491 (2016).
[15] S. Westenhoff, D. Palecek, P. Edlund, P. Smith, and D. Zigmantas, J. Am. Chem. Soc. **134**, 16484 (2012).
[16] W. Kuehn, K. Reimann, M. Woerner, T. Elsaesser, and R. Hey, J. Phys. Chem. B **115**, 5448 (2011).
[17] M. Woerner, W. Kuehn, P. Bowlan, K. Reimann, and T. Elsaesser, New J. Phys. **15**, 025039 (2013).
[18] F. D. Fuller and J. P. Ogilvie, Annu. Rev. Phys. Chem. **66**, 667 (2015).
[19] T. A. A. Oliver, R. Soc. Open Sci. **5**, 171425 (2018).
[20] L. Zhou, L. Tian, and W. K. Zhang, Chin. J. Chem. Phys. **33**, 385 (2020).
[21] M. Cho, *Two-Dimensional Optical Spectroscopy*, Boca Raton: CRC Press, (2009).
[22] D. M. Jonas, Annu. Rev. Phys. Chem. **54**, 425 (2003).
[23] M. Cho, Chem. Rev. **108**, 1331 (2008).
[24] N. S. Ginsberg, Y. C. Cheng, and G. R. Fleming, Acc. Chem. Res. **42**, 1352 (2009).
[25] Z. Ganim, H. S. Chung, A. W. Smith, L. P. DeFlores, K. C. Jones, and A. Tokmakoff, Acc. Chem. Res. **41**, 432 (2008).
[26] D. Abramavicius, B. Palmieri, D. V. Voronine, F. Šanda, and S. Mukamel, Chem. Rev. **109**, 2350 (2009).
[27] S. Mukamel, Y. Tanimura and P. Hamm, Acc. Chem. Res. **42**, 1207(2009).
[28] B. Tobias, S. Jens, H. M. Vaswani, C. Minhaeng, R. E. Blankenship, and G. R. Fleming, Nature **434**, 625 (2005).
[29] G. S. Engel, T. R. Calhoun, E. L. Read, T. K. Ahn, T. Mancal, Y. C. Cheng, R. E. Blankenship, and G. R. Fleming, Nature **446**, 782 (2007).
[30] L. Hohjai, C. Yuan-Chung, and G. R. Fleming, Science **316**, 1462 (2007).
[31] E. Collini, C. Y. Wong, K. E. Wilk, P. M. Curmi, P. Brumer, and G. D. Scholes, Nature **463**, 644 (2010).
[32] F. D. Fuller, J. Pan, A. Gelzinis, V. Butkus, S. S. Senlik, D. E. Wilcox, C. F. Yocum, L. Valkunas, D. Abramavicius, and J. P. Ogilvie, Nat. Chem. **6**, 706 (2014).
[33] T. R. Calhoun, N. S. Ginsberg, G. S. Schlau-Cohen, Y. C. Cheng, M. Ballottari, R. Bassi, and G. R. Fleming, J. Phys. Chem. B **113**, 16291 (2009).
[34] G. Panitchayangkoon, D. Hayes, K. A. Fransted, J. R. Caram, E. Harel, J. Wen, R. E. Blankenship, and G. S. Engel, Proc. Natl. Acad. Sci. USA **107**, 12766 (2010).
[35] J. Lim, D. Palecek, F. Caycedo-Soler, C. N. Lincoln, J. Prior, H. von Berlepsch, S. F. Huelga, M. B. Plenio, D. Zigmantas, and J. Hauer, Nat. Commun. **6**, 7755 (2015).
[36] J. M. Richter, F. Branchi, V. D. A. C. Franco, B. Zhao, R. H. Friend, G. Cerullo, and F. Deschler, Nat. Commun. **8**, 376 (2017).
[37] A. Jha, H. G. Duan, V. Tiwari, P. K. Nayak, H. J. Snaith, M. Thorwart, and R. J. D. Miller, ACS Photon. **5**, 852 (2018).
[38] K. W. Stone, G. Kenan, D. B. Turner, L. Xiaoqin, S. T. Cundiff, and K. A. Nelson, Science **324**, 1169 (2009).
[39] D. B. Turner and K. A. Nelson, Nature **466**, 1089 (2010).
[40] A. E. Almand-Hunter, H. Li, S. T. Cundiff, M. Mootz, M. Kira, and S. W. Koch, Nature **506**, 471 (2014).
[41] S. Yue, Z. Wang, X. C. He, G. B. Zhu, and Y. X. Weng, Chin. J. Chem. Phys. **28**, 509 (2015).
[42] T. Brixner, I. V. Stiopkin, and G. R. Fleming, Opt. Lett. **29**, 884 (2004).
[43] T. Brixner, T. Mancal, I. V. Stiopkin, and G. R. Fleming, J. Chem. Phys. **121**, 4221 (2004).
[44] M. L. Cowan, J. P. Ogilvie, and R. J. D. Miller, Chem. Phys. Lett. **386**, 184 (2004).
[45] A. Ramünas and Z. Donatas, Opt. Express **19**, 13126 (2011).
[46] X. Ma, J. Dostal, and T. Brixner, Opt. Express **24**, 20781 (2016).
[47] Y. X. Weng, Chin. J. Chem. Phys. **31**, 135 (2018).
[48] E. M. Grumstrup, S. H. Shim, M. A. Montgomery, N. H. Damrauer, and M. T. Zanni, Opt. Express **15**, 16681 (2007).
[49] J. A. Myers, K. L. M. Lewis, P. F. Tekavec, and J. P. Ogilvie, Opt. Express **16**, 17420 (2008).
[50] K. Gundogdu, K. W. Stone, D. B. Turner, and K. A. Nelson, Chem. Phys. **341**, 89 (2007).
[51] J. C. Vaughan, T. Hornung, K. W. Stone, and K. A. Nelson, J. Phys. Chem. A **111**, 4873 (2007).
[52] K. W. Stone, D. B. Turner, G. Kenan, S. T. Cundiff, and K. A. Nelson, Acc. Chem. Res. **42**, 1452 (2009).
[53] D. B. Turner, K. W. Stone, K. Gundogdu, and K. A. Nelson, Rev. Sci. Instrum. **82**, 307 (2011).
[54] D. Brida, C. Manzoni, and G. Cerullo, Opt. Lett. **37**, 3027 (2012).
[55] J. Rehault, M. Maiuri, A. Oriana, and G. Cerullo, Rev. Sci. Instrum. **85**, 123107 (2014).
[56] J. D. Hybl, A. W. Albrecht, S. M. G. Faeder, and D. M. Jonas, Chem. Phys. Lett. **297**, 307 (1998).
[57] L. Lepetit and M. Joffre, Opt. Lett. **21**, 564 (1996).
[58] A. D. Bristow, D. Karaiskaj, X. Dai, T. Zhang, C. Carlsson, K. R. Hagen, R. Jimenez, and S. T. Cundiff, Rev. Sci. Instrum. **80**, 073108 (2009).
[59] X. Li, T. Zhang, C. N. Borca, and S. T. Cundiff, Phys. Rev. Lett. **96**, 057406 (2006).
[60] T. Zhang, I. Kuznetsova, T. Meier, X. Li, R. P. Mirin,

DOI:10.1063/1674-0068/cjcp2012222

P. Thomas, and S. T. Cundiff, Proc. Natl. Acad. Sci. USA **104**, 14227 (2007).
[61] D. Xingcan, R. Marten, L. Hebin, A. D. Bristow, F. Cyril, M. Shaul, and S. T. Cundiff, Phys. Rev. Lett. **108**, 193201 (2012).
[62] T. L. Courtney, S. D. Park, R. J. Hill, B. Cho, and D. M. Jonas, Opt. Lett. **39**, 513 (2014).
[63] W. Zhu, R. Wang, C. Zhang, G. Wang, Y. Liu, W. Zhao, X. Dai, X. Wang, G. Cerullo, S. Cundiff, and M. Xiao, Opt. Express **25**, 21115 (2017).
[64] T. Peifang, K. Dorine, S. Yoshifumi, and W. S. Warren, Science **300**, 1553 (2003).
[65] W. Wagner, C. Li, J. Semmlow, and W. S. Warren, Opt. Express **13**, 3697 (2005).
[66] A. K. De, D. Monahan, J. M. Dawlaty, and G. R. Fleming, J. Chem. Phys. **140**, 194201 (2014).
[67] P. F. Tekavec, G. A. Lott, and A. H. Marcus, J. Chem. Phys. **127**, 214307 (2007).
[68] V. Tiwari, Y. A. Matutes, A. T. Gardiner, T. L. C. Jansen, R. J. Cogdell, and J. P. Ogilvie, Nat. Commun. **9**, 4219 (2018).
[69] S. Goetz, D. Li, V. Kolb, J. Pflaum, and T. Brixner, Opt. Express **26**, 3915 (2018).
[70] S. Draeger, S. Roeding, and T. Brixner, Opt. Express **25**, 3259 (2017).
[71] K. J. Karki, J. R. Widom, J. Seibt, I. Moody, M. C. Lonergan, T. Pullerits, and A. H. Marcus, Nat. Commun. **5**, 5869 (2014).
[72] G. Nardin, T. M. Autry, K. L. Silverman, and S. T. Cundiff, Opt. Express **21**, 28617 (2013).
[73] E. Vella, H. Li, P. Grégoire, S. M. Tuladhar, and E. R. Bittner, Sci. Rep. **6**, 29437 (2016).
[74] M. Aeschlimann, T. Brixner, D. Differt, U. Heinzmann, M. Hensen, C. Kramer, F. Lkermann, P. Melchior, W. Pfeiffer, M. Piecuch, C. Schneider, H. Stiebig, C. Strüber, and P. Thielen, Nat. Photon. **9**, 663 (2015).
[75] S. Rahav and S. Mukamel, Phys. Rev. A **81**, 063810 (2010).
[76] M. Aeschlimann, T. Brixner, A. Fischer, C. Kramer, P. Melchior, W. Pfeiffer, C. Schneider, C. Struber, P. Tuchscherer, and D. V. Voronine, Science **333**, 1723 (2011).
[77] C. Timm and K. H. Bennemann, J. Phys. Conden. Matt. **16**, 661 (2004).
[78] H. S. Tan, J. Chem. Phys. **129**, 124501 (2008).
[79] S. Goetz, D. Li, V. Kolb, J. Pflaum, and T. Brixner, Opt. Express **26**, 3915 (2018).
[80] S. Mueller and T. Brixner, J. Phys. Chem. Lett. **11**, 5139 (2020).
[81] I. Coddington, N. Newbury, and W. Swann, Optica **3**, 414 (2016).
[82] I. Coddington, W. C. Swann, and N. R. Newbury, Phys. Rev. Lett. **100**, 013902 (2008).
[83] K. Fritz, G. Christoph, and H. Ronald, Opt. Lett. **29**, 1542 (2004).
[84] B. Lomsadze and S. T. Cundiff, Opt. Lett. **42**, 2346 (2017).
[85] B. Lomsadze and S. T. Cundiff, Science **357**, 1389 (2017).
[86] P. A. Elzinga, F. E. Lytle, Y. Jian, G. B. King, and N. M. Laurendeau, Appl. Spec. **41**, 2 (1987).
[87] B. Lomsadze, B. C. Smith, and S. T. Cundiff, Nat. Photon. **12**, 676 (2018).
[88] B. Lomsadze and S. T. Cundiff, IEEE Photon. Tech. Lett. **31**, 1886 (2019).
[89] J. Jeon, J. W. Kim, T. H. Yoon, and M. Cho, J. Opt. Soc. Am. B **36**, 223 (2019).

DOI:10.1063/1674-0068/cjcp2012222